Journal of Arid Environments (1997) **37**: 251–260

Estimation of daily soil water evaporation using an artificial neural network

Huien Han & Peter Felker*

Center for Semi-Arid Forest Resources, Caesar Kleberg Wildlife Research Institute, Texas A&M University — Kingsville, Kingsville, TX 78363, U.S.A.

(*Received 25 September 1996, accepted 3 April 1997*)

In field water balance studies, one of the major difficulties is the separation of evapo-transpiration into plant transpiration and soil evaporation. In this paper, the radial basis function (RBF) neural network was implemented using C language to estimate daily soil water evaporation from average relative air humidity, air temperature, wind speed and soil water content in a cactus field study. The RBF neural network learned rapidly and converged after about 1000 training iterations. The optimum number of hidden neurons was found to be six. The RBF neural network achieved good agreement between predicted and measured values. The average absolute percent error and the root mean squared error was 21·0% and 0·17 mm for the RBF neural network *vs*. 30·1% and 0·28 mm for the multiple linear regression (MLR). The RBF neural network technique appears to be an improvement over the MLR technique for estimating soil evaporation.

Keywords: water use efficiency; cacti; transpiration

Introduction

In field water balance studies to determine plant water use, one of the major difficulties is the separation of evapo-transpiration into plant transpiration and soil evaporation (Fisher & Turner, 1978; Boast, 1986). Evapo-transpiration can be determined by subtracting the change of water stored in the soil profile using neutron scattering method (Heitholt, 1989), and surface runoff collected or measured with weirs and deep drainage, from the amount of precipitation for a given period of time (Bannister, 1986). Both plant transpiration and soil evaporation, however, are difficult to determine in the field. A review of literature by Boast (1986) and Bannister (1986) suggested the determination of soil evaporation was easier and less costly than determination of plant transpiration. Therefore, soil evaporation is usually estimated to partition evapo-transpiration into soil evaporation and plant transpiration. Thus, the determination of soil evaporation is one of the most important parameters that impacts water balance studies.

*Corresponding author.

0140–1963/97/020251 + 10 $25.00/0/ae970269

Soil evaporation can be either directly measured or indirectly estimated. Klocke *et al.* (1985, 1990), Shawcraft & Gardner (1983) and Boast & Robertson (1982) used a large-scale lysimeter, minilysimeters or microlysimeters to measure daily soil evaporation. These direct measurements were accurate but costly and time consuming.

Indirect methods developed so far employ mathematical models to predict soil water evaporation from either nearly saturated soils (stage 1) or non-saturated soils (stage 2) (Ritchie, 1972; Al-Khafaf *et al.*, 1978; Idso *et al.*, 1979). Energy-based mathematical models using inputs such as net radiation, evaporative demand, soil water status, plant canopy conditions etc., have been used to predict soil water evaporation under stage 1 conditions when the soil surface was near saturation. In contrast, mathematical models used to predict soil water evaporation when the soil surface is no longer saturated (stage 2) do not use energy or climatic data. Typically, stage 2 models are determined empirically, and relate declining soil water evaporation rates after saturated soil water conditions to time with an exponential decay function (Ritchie, 1972; Al-Khafaf *et al.*, 1978; Idso *et al.*, 1979).

For example, Ritchie (1972) developed an empirical energy-based model in which net radiation, air temperature and leaf area index were used to predict daily soil evaporation from a row crop field. Idso *et al.* (1979) also developed an empirical energy-based model in which daily net solar radiation, daily net thermal radiation and soil albedo were used to estimate daily soil evaporation from the bare soil. Al-Khafaf *et al.* (1978) described two mathematical models that were used in a combined manner to estimate daily soil evaporation after rainfall or irrigation.

Under semi-arid, non-irrigated conditions, many rainfall events are not sufficiently great to bring soil back to saturated stage 1 conditions. Under these circumstances it is difficult to know whether to use models for stage 1 or stage 2 conditions. Thus it would be useful to have a more general model in which it was not necessary to specify whether one was operating under stage 1 or stage 2 conditions.

Artificial neural networks, derived from the structure and functioning of the human brain, have been used in a broad range of applications including pattern recognition, classification, function approximation and automatic control (McAvoy *et al.*, 1989; Leonard *et al.*, 1992; Rao & Gupta, 1993). In this paper, we employ the radial basis function (RBF) neural network technique to estimate soil evaporation from a 3-year-old cactus plantation in a semi-arid region, and compare this new technique with a more conventional multiple linear regression (MLR) technique.

Methods and materials

Data was obtained in a 3-year-old experimental planting on a 1·0 m × 1·5 m spacing of slow-growing but cold-hardy spineless *Opuntia ellisiana* selection (Han & Felker, 1996). The non-irrigated field trial was located in a semi-arid, subtropical region of Texas. The leaf area index was 2·02 on 15 April 1994 when new cladodes were emerging. By 15 May 1994, when this study began, the new cladodes were well developed. On 15 April 1995 the leaf area index was 3·08. This study ended on 15 February 1995. The leaf area index showed only a small change during the course of this study. The effect of plant canopy conditions on soil evaporation, therefore, was limited. The factors considered in this study include air relative humidity, air temperature, wind speed and soil water content.

Measurement of soil evaporation and soil water content

Soil evaporation was measured using the microlysimeter technique (Boast & Robertson, 1982; Shawcroft & Gardner, 1983). The microlysimeters, 10 cm long and

4·9 cm in diameter, were made of 2-mm thick aluminum pipe. The portable electronic balance, used to weigh the microlysimeters, had an accuracy of 0·1 g (0·05 mm of water). The microlysimeters were weighed daily at about 0830h CDT.

Two lysimeters were placed between the row and two under the plant canopy, and the four lysimeters were replaced every day. The daily soil evaporation rate was obtained by averaging the measured soil evaporation rate from the four lysimeters.

To account for seasonal variations in meteorological factors and soil evaporation, daily microlysimeter samplings were conducted over an approximate 15-day period in the spring (May–June 1994), summer (July–Aug 1994), fall (Oct–Nov 1994) and Winter (Jan–Feb 1995). While no measurable rainfall occurred during the 15-day periods, a 60 mm rain occurred 1 day before the May–June 1994 period that brought the volumetric water content (31%) to near field capacity (35%) and allowed a determination of water evaporation under near stage 1 conditions.

Associated with each microlysimeter measurement, gravimetric soil water content (top 10 cm) was obtained at a site adjacent to the microlysimeter location. Three gravimetric soil samples were taken with a hand probe immediately after weighing the microlysimeters. Average gravimetric soil water content over the three samples was obtained and used.

Collection of meteorological data

Daily average air temperature, relative humidity and wind speed were obtained from the Texas A&M University Research and Extension Center at Corpus Christi, about 40 km away.

Radial basis function neural network

Artificial neural networks contain highly interconnected and interacting units (neurons) (Haykin, 1994). The artificial neural networks accept a set of inputs (an input vector) from which a corresponding set of outputs (an output vector) is produced (Wasserman, 1993). In this paper, the radial basis function (RBF) neural network was chosen because of its rapid learning and generality (Wasserman, 1993). By generality, we mean that the network can produce the correct output vector despite significant variations between the input vector and the input vectors used during training (Leonard *et al*., 1992).

An RBF neural network is a multi-layer network whose output nodes form a linear combination of the basis functions computed by the hidden layer nodes (Hush & Horne, 1993). The architecture of the multi-layer neural network chosen in this study, depicted in Fig. 1, consists of three layers: the input layer, the output layer and a hidden layer. The input layer contains four neurons which receive input signals of relative air humidity (x_1), air temperature (x_2), wind speed (x_3) and gravimetric soil water content (x_4). The output layer contains one neuron which produces a corresponding output, i.e. daily soil evaporation (y), for a given input vector. The number of neurons in the hidden layer significantly affects the network performance. The optimum number of neurons in the hidden layer is determined by the inherent relationship between the input vectors and the output vectors.

All neurons are fully-connected in a feed-forward fashion. More specifically, each neuron in a given layer is connected to each neuron in the layer directly above it by an associated numerical connection weight.

The input neurons simply pass the input signal to each hidden neuron and perform no computation. The hidden neurons first compute the Euclidean distance between the input vector and the connection weight vector. Then, the output (activation level)

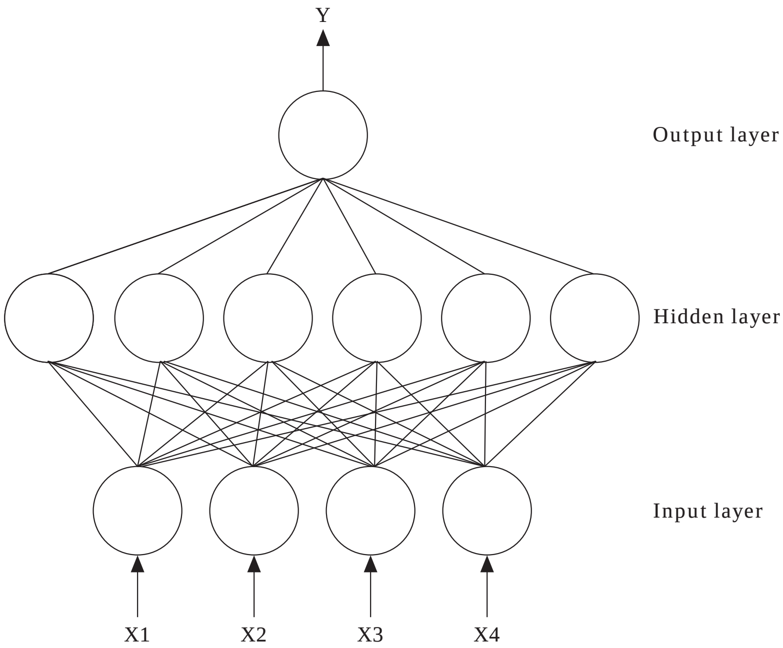

Figure 1. Architecture of the multi-layer neural network.

of the hidden neurons is calculated by the Gaussian function (also called a basis function) of the form (Hush & Horne, 1993; Wasserman, 1993):

$$\boldsymbol{\mu}_{h.j} = \exp[-\frac{(X-W_{h.j})^T\ (X-W_{h.j})}{2\boldsymbol{\sigma}^2_{h.j}}]j = 1,\ 2,\ .\ .\ .\ ,\ n$$

where $\boldsymbol{\mu}_{\mathrm{h.j}}$ is the output of the jth neuron in the hidden layer ('h' indicates the hidden layer); X is the input vector; $W_{\mathrm{h.j}}$ is the centroid of the jth hidden neuron (Park & Sandberg, 1991) or the weight vector for the jth hidden neuron to the input neurons (Hush & Horne, 1993); $\boldsymbol{\sigma}_{\mathrm{h,j}}$ is the normalization parameter for the jth hidden neuron; 'T' indicates the transpose operation; and n is the number of hidden neurons.

The outputs of the hidden neurons are in the range from 0 to 1. The closer the input is to the centroid of the hidden neurons, the larger the response of the hidden neurons. The output neuron produces the output for a given input vector by forming a weighted linear combination of the outputs from the hidden neurons. The output layer neuron equation is given (Hush & Horne, 1993; Wasserman, 1993):

$$y = W^T{}_o\boldsymbol{\mu}_h$$

where y is the output of the output neuron, W_o is the weight vector for this output neuron and $\boldsymbol{\mu}_{\mathrm{h}}$ is the vector of outputs from the hidden layer. 'T' indicates the transpose operation. The overall network performs a non-linear transformation by forming a linear combination of the non-linear basis functions.

For an RBF neural network to map a specific input vector to target output it must be trained based on a set of known input–output pairs. All connection weights are adjusted according to certain learning rules during the training process. The inherent relationship between the input signals and the output signal(s) is stored in these connection weights.

The RBF learning process is broken into two stages: learning in the hidden layer, followed by learning in the output layer. Learning in the hidden layer is performed using a K_MEANS clustering algorithm (Lee, 1991; Hush & Horne, 1993), and learning in the output layer is performed using a Least Mean Square (LMS) algorithm (Hush & Horne, 1993).

During the first stage, the connection weights between the input neurons and the hidden neurons, i.e. the centroid of the hidden neurons, and the normalization parameters for each hidden neuron are determined. Once the clustering algorithm is complete, the normalization parameter ($\sigma_{h,j}$) is calculated as:

$$\sigma^2_{h.j} = \frac{1}{m_{h.j}} \sum_{X \in \theta_{h.j}} (X - W_{h.j})^T (X - W_{h.j})$$

where $\theta_{h.j}$ is the set of training input vectors (X) grouped with the centroid of the jth hidden neuron ($W_{h.j}$), and $m_{h.j}$ is the number of the training input vectors in $\theta_{h.j}$.

During the second stage, the connection weight between the hidden neurons and the output neuron are determined. The K_MEANS and LMS algorithms were described in detail by Hush & Horne (1993). The C programming language implementation of these algorithms can be obtained from the senior author.

Soil evaporation prediction by regression technique

Least square error fitting was conducted using the SAS statistical software package to determine the multiple linear regression equation.

Results and discussion

The data set consisting of 53 input–output pairs from the experiment described above was randomly split into a training set and a test set. The training set had 40 input–output pairs and the test set 13 input–output pairs. Table 1 shows some statistics of the training set.

To improve the neural network performance, each component of the input vector in both the training set and the test set was normalized by the following procedure: the corresponding component of the mean vector (Table 1) was subtracted from each component of the input vector and this difference was divided by the corresponding component of the standard deviation vector (Table 1). The training data set was used to adjust the connection weight. The test data set was used to test the performance of the neural network.

Table 1. *Simple statistics of the data set used to train the RBF neural network to predict daily soil evaporation (* N = 40*)*

Factors	Mean	S.D.	Minimum	Maximum
Relative humidity (%)	76·91	10·01	56·49	96·27
Air temp. (°C)	22·30	6·63	9·17	30·00
Wind speed (km h^{-1})	11·28	4·23	4·93	21·46
Top 10 cm soil water content (g g^{-1})	0·084	0·026	0·040	0·172
Daily soil evaporation (mm)	0·73	0·57	0·19	2·44

Determining the required number of training iterations and optimum number of the hidden neurons

The root mean squared error (SE) for the test data set was used to evaluate the performance of the neural network. The test data set is shown in Table 2. The SE is defined as:

$$SE = \left(\frac{\sum(Y_m - Y_p)^2}{n}\right)^{\frac{1}{2}}$$

where Y_m is the measured soil evaporation, Y_p is the predicted soil evaporation and n is the number of the input vector in the test data set (n = 13).

Figure 2 gives a plot of SE *vs.* the logarithm of the number of training iterations to the base 10 in the second stage when the number of the hidden neurons is five. The network learns rapidly since the network has converged after 1000 iterations.

In theory, the RBF neural network is capable of forming an arbitrarily close approximation to any continuous non-linear mapping (Park & Sandberg, 1991). For a given input–output space, the number of hidden layers and the number of neurons in the hidden layer significantly affects the performance of the neural network (Li *et al.*, 1993). Figure 3 gives a plot of SE *vs.* the number of hidden neurons for a converged network (with 1200 training iterations). As computation time increases dramatically with the number of hidden neurons, it was determined that six hidden neurons were optimum.

The performance of the RBF neural network and multiple linear regression

The predicted soil evaporation shown in Table 2 was obtained from the converged RBF neural network with six hidden neurons. Good agreement between measured and predicted value was achieved since the average, maximum and minimum absolute percent error was 21·0%, 49·6% and 1·9%. The root mean squared error was 0·17 mm.

To compare the RBF neural network with MLR, the same 40 input–output pairs in the normalized training data set were used to obtain the following regression equation:

$$Y_p = 0{\cdot}726 - 0{\cdot}054x_1 + 0{\cdot}181x_2 + 0{\cdot}057x_3 + 0{\cdot}549x_4 \; (R^2 = 0{\cdot}76)$$

where $\mathbf{Y_p}$ is the predicted daily soil evapo-transpiration (mm), x_1 is the average relative air humidity (%), x_2 is the average air temperature (°C), x_3 is the average wind speed (km h^{-1}) and x_4 is the gravimetric soil water content (g g^{-1}).

The same 13 input–output pairs were used to test the performance of the MLR. From Table 2, the average, maximum and minimum absolute percent error were found to be 30·1%, 95·1% and 2·0%, respectively. The root mean squared error was 0·28 mm.

It can be seen that the RBF neural network in this study had a lower absolute percent error and root mean squared error in predicting soil evaporation than did multiple linear regression technique.

On theoretical grounds, we believe our neural net model containing energy (temperature, wind speed and humidity) terms and gravimetric moisture terms is more applicable on a year round basis than hybrid stage 1/stage 2 model of Ritchie (1972). Essentially, Ritchie's choice of stage 1 or stage 2 conditions depends on whether soil water evaporation is more dependent on available energy (stage 1) or hydraulic capabilities (stage 2) of the soil to deliver water to the soil surface. Under stage 2 conditions Ritchie's model only uses an empirical determination of a hydraulic

Table 2. *Test data set, measured soil evaporation and predicted soil evaporation using both RBF neural network and multiple linear regression*

No.	Relative humidity (%)	Air temp. (°C)	Wind speed (km h^{-1})	Soil water content (g g^{-1})	Y_m* (mm)	Y_p† (mm)		APE‡ (%)	
						RBF	MLR	RBF	MLR
1	88·80	23·86	11·80	0·148	1·58	1·75	2·05	11·09	29·66
2	74·26	22·41	4·12	0·116	1·04	1·27	1·31	22·49	26·79
3	78·92	24·17	8·13	0·084	0·58	0·29	0·73	49·56	25·46
4	86·20	28·47	8·81	0·097	0·96	1·04	1·09	8·72	12·97
5	82·73	27·56	5·96	0·083	0·74	0·58	0·75	20·98	1·97
6	79·89	27·86	11·22	0·051	0·37	0·25	0·18	31·89	52·09
7	80·93	28·61	13·73	0·051	0·32	0·43	0·23	34·98	28·87
8	87·12	19·59	18·74	0·090	0·42	0·55	0·83	29·36	95·09
9	86·56	28·83	6·81	0·108	1·51	1·57	1·30	3·68	14·23
10	85·62	24·88	4·93	0·122	2·13	2·00	1·46	6·51	31·63
11	80·47	28·33	14·39	0·051	0·41	0·44	0·23	7·04	43·45
12	67·17	13·07	14·20	0·098	0·77	1·12	0·86	44·71	11·44
13	83·46	25·17	5·22	0·128	1·93	1·97	1·61	1·94	16·77

*Measured soil evaporation.
†Predicted soil evaporation.
‡Absolute percent error.

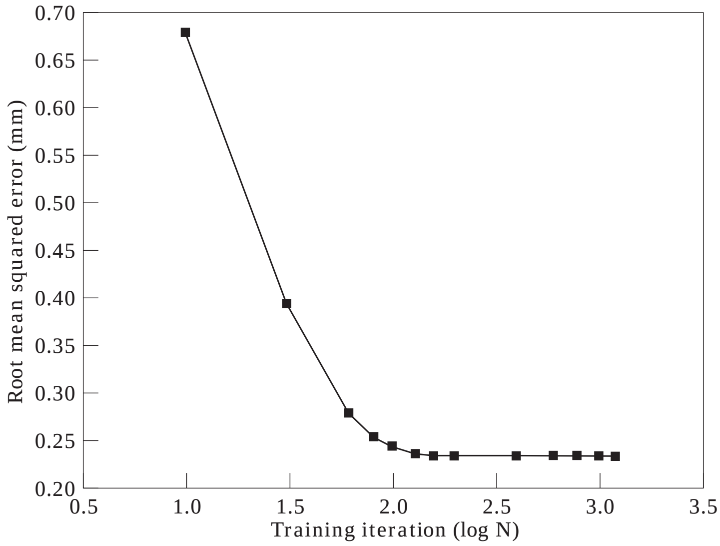

Figure 2. Predicted root mean squared error *vs.* training iterations.

conductivity term (alpha) from a drying cycle and the square root of the time. Certainly in a single summer's growing season when the evaporative demand greatly exceeded the soils hydraulic ability to deliver water to the soil surface, use of a single constant alpha seems warranted. However, on non-frozen soils in winter months, it would appear possible that the available energy for evaporation could be less than or equal to the soil's water hydraulic conductivity properties. Under this scenario, energy terms could again be important in predicting soil water evaporation and it would be necessary to recalculate the alpha term under the new energy balance/soil hydraulic conductivity scenario. As we have demonstrated with RBF neural net technique, this is not necessary for year round prediction of soil water evaporation. An added

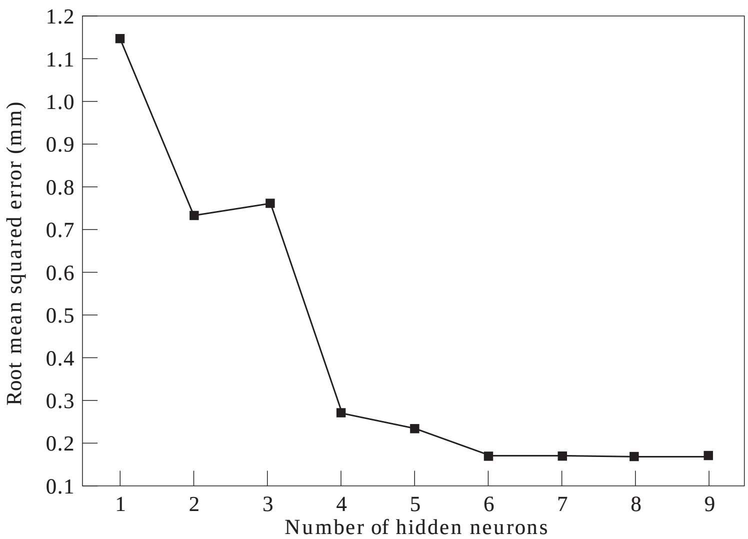

Figure 3. Predicted root mean squared error *vs.* number of hidden neurons.

advantage of our model is that it uses easily obtainable climatic data in conjunction with easy to measure gravimetric soil moisture contents.

It has been difficult to compare the output of our model to those of Ritchie (1972), Idso *et al*. (1979) and Al-Khafaf *et al*. (1978) since the previous models focused primarily on stage 1 soil water evaporation. We did compare the output of our model with Al-Khafaf's stage 2 model over a 12-day period (stage 2) in June 1994. The parameters in Al-Khafaf's stage 2 model shown below were determined using our data obtained during a 15-day period in May 1994 in which 60 mm of rain occurred 2 days before we began our measurements. By curve fitting the data, the parameters a and b were found to be 1·08 mm $day^{-0·7}$ and 0·7, respectively.

$$E_s = at^b$$

where E_s is the cumulative soil evaporation since the beginning of stage 2 and t is the days elapsed since stage 2 begins.

A comparison of our RBF model and that of Al-Khafaf during a drying cycle in June 1994 revealed that our model had a slightly higher root mean squared error of 0·11 mm as compared to a root mean squared error from Al-Khafaf's model (Al-Khafaf *et al*., 1978) of 0·08 mm. However, as we noted above, the stage 2 model of Al-Khafaf *et al*. (1978) would have to be recalibrated for use in drastically different seasons while this is not necessary for our RBF model.

While Idso *et al*. (1979) developed a single equation to calculate daily soil evaporation rates during all three stages of soil drying, it was still necessary to decide which phase was operative at a given point in time for year round daily soil evaporation.

To illustrate the utility of our RBF neural network model, we used it to estimate yearly soil evaporation and thus separate transpiration from evapo-transpiration in a 4-year study to measure the water-use efficiency of *Opuntia ellisiana*. We obtained soil evaporation estimates of 249 mm in 1993 and 214 mm in 1994 and a water-use efficiency of 162 kg water kg^{-1} dry matter (Han & Felker, 1996).

The RBF neural network (and artificial neural network techniques in general) offers significant advantages over the MLR and other conventional methods in predicting soil evaporation because it is not necessary to specify the form of the mathematical model before fitting the data. This is important since many agronomic system processes have multiple factors that change with time. As a result it is often difficult to find an appropriate mathematical model to describe these processes. While this particular neural network will have to be tested against other models and with data sets from widely varying climatic and geographical regions, we feel this neural network is a promising technique to help in understanding processes in complicated and dynamic agronomic systems.

We gratefully acknowledge financial assistance from the U.S. Agency for International Development Grant DHR-5542-G-SS-9032. Publication number 97-116 of the Caesar Kleberg Wildlife Research Institute.

References

Al-Khafaf, S., Wierenga, P.J. & Williams, B.C. (1978). Evaporative flux from irrigated cotton as related to leaf area index, soil water and evaporative demand. *Agronomy Journal*, **70**: 912–917.

Bannister, P. (1986). Water relation and stress. In: Moore, P.D. & Chapman, S.B. (Eds), *Methods in Plant Ecology* (2nd Edn), pp. 73–143. Oxford: Blackwell Scientific Publications. 589 pp.

Boast, C.W. (1986). Evaporation from bare soil measured with high spatial resolution. In: Klute A (Ed.), *Methods of Soil Analysis* — Part I, pp. 889–900. Madison, W.I.: American Society of Agronomy and Soil Science Society of America. 1216 pp.

Boast, C.W. & Robertson, T.M. (1982). A 'micro-lysimeter' method for determining evaporation from bare soil: description and laboratory evaluation. *Soil Science Society of America Journal*, **46**: 689–696.

Fisher, R.A. & Turner, N.C. (1978). Plant productivity in the arid and semi-arid zones. *Annual Review of Plant Physiology*, **29**: 277–317.

Han, H. & Felker, P. (1996). Field validation of water-use efficiency of the CAM plant *Opuntia ellisiana* in south Texas. *Journal of Arid Environments*, **36**: 133–148.

Haykin, S. (1994). *Neural Networks: A comprehensive foundation*. New York: Macmillan College Publishing Company. 691 pp.

Heitholt, J.J. (1989). Water use efficiency and dry matter distribution in nitrogen- and water-stressed wheat. *Agronomy Journal*, **81**: 464–469.

Hush, D.R. & Horne, B.G. (1993). Progress in supervised neural networks. *IEEE Signal Processing Magazine*, **10**(1): 8–39.

Idso, S.B., Reginato, R.J. & Jackson, R.D. (1979). Calculation of evaporation during the three stages of soil drying. *Water Resources Research*, **15**: 487–488.

Klocke, N.L., Heermann, D.F. & Duke, H.K. (1985). Measurement of evaporation and transpiration with lysimeter. *Transactions of the ASAE*, **28**: 183–192.

Klocke, N.L., Martin, D.L., Todd, R.W., Dehaan, D.L. & Polymenopoulos AD. (1990). Evaporation measurements and predictions from soils under crop canopies. *Transactions of the ASAE*, **33**: 1590–1596.

Lee, Y. (1991). Handwritten digit recognition using K nearest-neighbor, radial-basis function, and backpropagation neural networks. *Neural Computation*, **3**: 440–449.

Leonard, J.A., Kramer, M.A. & Ungar, L.H. (1992). Using radial basis functions to approximate a function and its error bounds. *IEEE Transactions on Neural Networks*, **3**: 624–627.

Li, Z., Cheng, Z, Xu, L. & Li, T. (1993). Nonlinear fitting by using a neural net algorithm. *Analytical Chemistry*, **65**: 393–396.

McAvoy, T.J., Wang, N.S., Naidu, S., Bhat, N., Gunter, J. & Simmons, M. (1989). Interpreting biosensor data via backpropagation. *IEEE International Neural Network Conference in 1989*, **I**: 227–233.

Park, J. & Sandberg, I.W. (1991). Universal approximation using radial-basis-function networks. *Neural Computation*, **3**: 246–257.

Rao, D.H. & Gupta, M.M. (1993). Dynamic neural controller with somatic adaptation. *IEEE International Conference on Neural Networks in 1993*, **I**: 558–563.

Ritchie, J.T. (1972). Model for predicting evaporation from a row crop with incomplete cover. *Water Resource Research*, **8**: 1204–1213.

Shawcroft, R.W. & Gardner, H.R. (1983). Direct evaporation from soil under a row crop canopy. *Agricultural Meteorology*, **28**: 229–238.

Wasserman, P.D. (1993). *Advanced Methods in Neural Computing*. New York: Van Nostrand Reinhold. 235 pp.